

p -SHELL NUCLEI AND TWO-FREQUENCY SHELL MODEL WITH A REALISTIC EFFECTIVE INTERACTION

A. GARGANO, L. CORAGGIO, A. COVELLO AND N. ITACO

*Dipartimento di Scienze Fisiche, Università di Napoli Federico II
and Istituto Nazionale di Fisica Nucleare*

Complesso Universitario di Monte S. Angelo, Via Cintia, 80126 Napoli, Italy

T. T. S. KUO

Department of Physics, SUNY, Stony Brook, New York 11794, USA

We have studied p -shell nuclei using a two-frequency shell-model approach with an effective interaction derived from the Bonn-A nucleon-nucleon potential by means of a G -matrix folded-diagram method. First, we briefly describe our derivation of the effective interaction in a model space composed of harmonic oscillator wave functions with two different length parameters, b_{in} and b_{out} , for the core and the valence orbits, respectively. Then we present some selected results of our calculations. We show that a good agreement with experiment is obtained, which is definitely better than that provided by a standard one-frequency calculation. A comparison with results obtained from large-basis shell-model calculations is also made.

1 Introduction

The p -shell nuclei have long been the subject of several theoretical investigations. In recent years, however, special interest in the study of these nuclei has been motivated by new relevant information on their structure. One of the main results has been the observation for some neutron-rich nuclei, such as ${}^6\text{He}$ and ${}^{11}\text{Li}$, of abnormally large interaction and reaction cross-sections.^{1,2} These nuclei have a very small one- and two-neutron separation energy and have been described as having a halo structure,³ namely an extended neutron distribution surrounding a tightly bound inner core. Generally, it has been observed that the p -shell nuclei have a rather extended density profile.

Within the framework of the standard shell-model, the description of these nuclei requires the use of multi-shell model spaces.⁴⁻⁶ In particular, large-basis no-core shell-model calculations have been performed⁶ making use of effective interactions derived from modern nucleon-nucleon (NN) potentials. The use of very large model spaces, however, makes in general the calculations quite complicated.

Recently, a two-frequency shell-model (TFSM) approach with a realistic G -matrix effective interaction has been developed^{7,8} to treat light nuclei near the drip lines. In this approach, the calculation of the effective interaction in-

volves use of harmonic oscillator wave functions of two different oscillator constants $\hbar\omega_{\text{in}}$ and $\hbar\omega_{\text{out}}$ for the core and valence orbits, respectively (the length parameters for these orbits will be denoted by b_{in} and b_{out} , $b = (\hbar/m\omega)^{1/2}$). This provides a simpler treatment of this kind of nuclei in that use of very large active spaces may be avoided. In fact, the effective interaction derived in the above way from the realistic NN potential should take into account the effects of correlations which are not explicitly included in the model space. We shall see in Sec. 3 that, in spite of its simplicity, the TFSM approach yields results which are quite satisfactory. Actually, it turns out that they are comparable to, or even better than, those obtained from large-basis shell-model calculations.

2 Two-Frequency Shell Model

In the TFSM approach the effective interaction V_{eff} is derived from the free NN potential by way of a G -matrix folded diagram method. This method has been developed within the framework of the ordinary (one-frequency) shell model and its description including a complete list of references can be found in Refs. 9 and 10. Here, we only give the essentials of the derivation of V_{eff} focusing attention on those features which are peculiar to the TFSM.

The first step for the derivation of V_{eff} is the choice of a closed core and the single-particle (sp) orbits over which the valence nucleons are distributed, that is the model space (usually referred to as P space) within which the effective interaction is derived. It should be noted here that V_{eff} is usually derived for two-valence particles or holes outside a doubly closed core. For instance, the P space for p -shell nuclei consists of a closed $(0s_{1/2})^4$ core with the two-valence nucleons confined in the $0p_{3/2}$ and $0p_{1/2}$ orbits. As usual, the P space is defined in terms of the eigenvectors of the harmonic oscillator. Within the TFSM approach, sp wave functions of two different length parameters b_{in} and b_{out} are used, the former for the inner core orbits and the latter for the outer valence orbits. Actually, as we shall see below, also orbits above the p shell come into play as intermediate states in the evaluation of the effective interaction. In this context, it should be noted that two sp wave functions with the same l and j values but different length parameters are in general not orthogonal. To assure the orthonormality condition for these states, in the present calculations we use b_{in} also for all outer orbits with $l = 0$.

At this point, V_{eff} could be derived for the chosen model space by means of a perturbation calculation in terms of the NN potential. However, the strong repulsive core contained in all realistic NN potential makes a perturbative treatment meaningless. This problem is overcome by introducing the reaction

matrix G . This matrix is defined by the integral equation ¹¹

$$G(\omega) = V + VQ_2 \frac{1}{\omega - Q_2 T Q_2} Q_2 G(\omega), \quad (1)$$

which can be solved in an essentially exact way by the matrix inversion method of Tsai-Kuo.¹² In Eq. (1) V represents the NN potential, T is the two-nucleon kinetic energy, and ω , commonly referred to as starting-energy, is the unperturbed energy of the interacting nucleons. The operator Q_2 is a two-body Pauli exclusion operator, whose complement $P_2 = (1 - Q_2)$ defines the space within which the G matrix is calculated. The role of Q_2 in Eq. (1) is to make sure that the intermediate states of G be outside this space. Note that plane-wave functions are employed for the intermediate states while Q_2 is defined in terms of harmonic oscillator wave functions as

$$Q_2 = \sum_{\text{all } ab} Q(ab) |ab\rangle \langle ab|, \quad (2)$$

where $Q(ab) = 0$, if $b \leq n_1$, $a \leq n_3$, or $b \leq n_2$, $a \leq n_2$, or $b \leq n_3$, $a \leq n_1$, and $Q(ab) = 1$ otherwise. The boundary of Q_2 is specified by the three numbers n_1 , n_2 , and n_3 , each representing a single-particle orbital (the orbits are numbered starting from the bottom of the oscillator well). In particular, n_1 is the number of orbitals below the Fermi surface of the doubly magic core, n_2 fixes the orbital above which the passive sp states start, and n_3 denotes the limit of the P_2 space.

It should be noted that in the calculation of G the space of active sp states, i.e. the number of levels between n_1 and n_2 , may be different from the model space within which V_{eff} is defined. Several arguments for choosing the former larger than the latter are given in Ref. 11. Generally, n_2 is fixed so as to include two major shell above the Fermi surface. In this paper we consider the p -shell nuclei with ${}^4\text{He}$ treated as core, thus we have $n_1 = 1$. Then we take $n_2 = 6$ so as to include all the five orbits of the p and sd shells above the Fermi surface. As regards the value of n_3 , it should be infinite, but in practice it is chosen to be a large but finite number. Namely, calculations are performed for increasing values of n_3 until numerical results become stable. For the present case we have found that a choice of $n_3 = 21$ turns out to be adequate.

From the above it is clear that the reaction matrix G , which depends on the space P_2 , is different for different choices of this space. As already discussed in the Introduction, in the TFMSM the choice of two different length

parameters, for the core and valence wave functions, seems to be appropriate to describe light nuclei such as those of the p shell. It poses, however, some technical difficulties in the calculation of the G matrix. In fact, transformations from two-particle states in the c.m. coordinates to those in the laboratory coordinates are not as easy to perform as in the case of a unique oscillator frequency. We have adopted an expansion procedure^{7,8} to surmount this problem. Namely, we expand the wave functions with b_{in} in terms of those with b_{out} , or vice versa.

Finally, using the above G matrix, we can now calculate V_{eff} in the chosen model space. This interaction, which is energy independent, can be written schematically in operator form as¹³

$$V_{\text{eff}} = \hat{Q} - \hat{Q}' \int \hat{Q} + \hat{Q}' \int \hat{Q} \int \hat{Q} - \hat{Q}' \int \hat{Q} \int \hat{Q} \int \hat{Q} + \dots, \quad (3)$$

where \hat{Q} (referred to as \hat{Q} -box) is a vertex function composed of irreducible linked diagrams in G , and the integral sign represents a generalized folding operation. \hat{Q}' is obtained from \hat{Q} by removing terms of first order in the reaction matrix G . After the \hat{Q} -box is calculated, V_{eff} is obtained by summing up the folded-diagram series (3) to all orders by means of the Lee-Suzuki iteration method.¹⁴ This last step can be performed in an essentially exact way for a given \hat{Q} -box.

As regards the calculation of the \hat{Q} -box, we need to make certain approximations, namely we include only diagrams through second order in G . They are precisely the seven first- and second-order diagrams considered by Shurpin *et al.*¹⁵ Higher-order diagrams might be important in some cases. For example, in Refs. 16 and 17 the role of third-order diagrams has been investigated within the framework of standard shell-model calculations. It was shown there that for the sd nuclei the third-order contributions lead to a change of about 10 – 15% in the effective interaction, while they reduce to only 5% or less for heavier nuclei (in this case only for the $T = 1$ matrix elements). In the TFMSM approach one may expect these higher-order diagrams are even less important. In fact, the magnitude of second order core-polarization diagrams, representing the most significant corrections to the G matrix, become rather small when the length parameter b_{out} becomes significantly larger than b_{in} .⁸ This is a consequence of the fact that when increasing b_{out} we are increasing the average distance between the core and valence nucleons, thus reducing the overlaps between them.

3 Results for p -Shell Nuclei

We present here some results of our calculations for the p -shell nuclei. They have been obtained by using the OXBASH shell model code.¹⁸

As already mentioned in the preceding section, we have assumed that the doubly magic ${}^4\text{He}$ is a closed core and let the valence particles occupy the two orbits $0p_{3/2}$ and $0p_{1/2}$. The spacing between these two levels, $\epsilon_{1/2} - \epsilon_{3/2}$, was fixed at 4.0 MeV, which corresponds to the excitation energy¹⁹ of the first $\frac{1}{2}^-$ state in ${}^5\text{He}$. This state, however, is a very broad resonance with a large error bar of about ± 1 MeV. For the sp energy $\epsilon_{3/2}$ we have taken the experimental one-neutron separation energy for ${}^5\text{He}$, 0.886 MeV.²⁰ The effective interaction was derived from the Bonn-A free NN potential²¹ following the procedure described in Sec. 2.

As regards the two length parameters b_{in} and b_{out} , the former was fixed⁷ at 1.45 fm while the latter was allowed to vary from 1.45 to 2.50 fm. To fix the value of b_{out} , we have calculated the ground-state energies for several nuclei with $6 \leq A \leq 8$. The corresponding binding energies have been then obtained by making use of the experimental ground-state binding energy²⁰ of ${}^4\text{He}$ and the Coulomb contributions taken from Ref. 22, where they were determined from a least-squares fit to experimental data.

In Table 1 we compare the experimental ground-state binding energies²⁰ with the calculated ones for three different values of b_{out} , 1.75, 2.00, and 2.25 fm. In the last column, labeled LBSM, we also report the results obtained from the large-basis shell-model calculations of Ref. 4. In this work, a complete $(0 + 2)\hbar\omega$ model space and an empirical effective interaction were used.²²

From Table 1 we see that the binding energies of the He isotopes and their corresponding mirror nuclei are well reproduced by using $b_{\text{out}} = 2.25$ fm. For these nuclei we overestimate the experimental values by about 0.5 MeV, which implies that a little larger b_{out} would be sufficient to reproduce them. As regards the other nuclei reported in Table 1, the value 2.0 fm gives a good agreement between theory and experiment. In particular, for ${}^6\text{Li}$ the experimental energy is overestimated by 0.360 MeV, while for ${}^7\text{Li}$ and ${}^7\text{Be}$ it is underestimated by about the same value. As regards ${}^8\text{Li}$ and ${}^8\text{B}$, the experimental binding energies are reproduced by the theory within few tens of keV. It should be noted that with the above choice of b_{out} the agreement between experiment and theory is comparable to, and in some cases better than, that obtained in Ref. 4.

We have then calculated the spectra and the electromagnetic properties of the nuclei reported in Table 1 using $b_{\text{out}} = 2.0$ and 2.25 fm for Li and He isotopes (and their corresponding mirror nuclei), respectively. It is worth

Table 1. Experimental and calculated ground-state binding energies (MeV). See text for details.

AZ	Expt	TFSM(1.75)	TFSM(2.00)	TFSM(2.25)	LBSM
${}^6\text{He}$	29.27	31.57	30.59	29.81	29.74
${}^6\text{Be}$	26.92	29.21	28.23	27.45	—
${}^6\text{Li}$	31.99	33.80	32.35	31.13	31.24
${}^7\text{He}$	28.82	31.25	30.17	29.32	—
${}^7\text{B}$	24.72	26.99	25.91	25.06	—
${}^7\text{Li}$	39.24	42.02	38.86	36.30	40.04
${}^7\text{Be}$	37.60	40.36	37.20	34.64	—
${}^8\text{He}$	31.41	35.61	33.57	31.91	31.24
${}^8\text{Li}$	41.28	45.07	41.23	38.16	41.54
${}^8\text{B}$	37.74	41.51	37.67	34.60	—

noting that we have not tried to adjust the value of b_{out} for each nucleus. The results obtained are in satisfactory agreement with the experimental data and will be reported in a forthcoming paper.²³ Here we shall only focus attention on ${}^8\text{Li}$. As regards the mirror nucleus ${}^8\text{B}$, only two excited states have been observed, one of them without spin-parity assignment.

In Fig. 1 the experimental and calculated spectra of ${}^8\text{Li}$ are compared. To evidence the scope of the TFMS, we also report the results we have obtained in a one-frequency shell-model calculation (OFMS)²⁴ as well as those of Ref. 4. In the OFMS calculations the length parameter, which is the same for the core and valence orbits, was fixed at 1.9 fm. This choice leads to a binding energy of 41.32 and 37.76 MeV for ${}^8\text{Li}$ and ${}^8\text{B}$, respectively.

From Fig. 1 we see that the three calculations give rise to the same levels, the OFMS and TFMS approaches producing also the same ordering. All the observed levels are predicted by the different calculations. They also yield, however, two more excited 2^+ states while for the 0^+ and 1_3^+ states only one experimental level with spin equal to 0 or 1 is available. All three calculations suggest that this state, which lies at 5.4 MeV, has $J^\pi = 1^+$ while for the (3) state at 6.1 MeV they predict $J^\pi = 3^+$. Regarding the quantitative

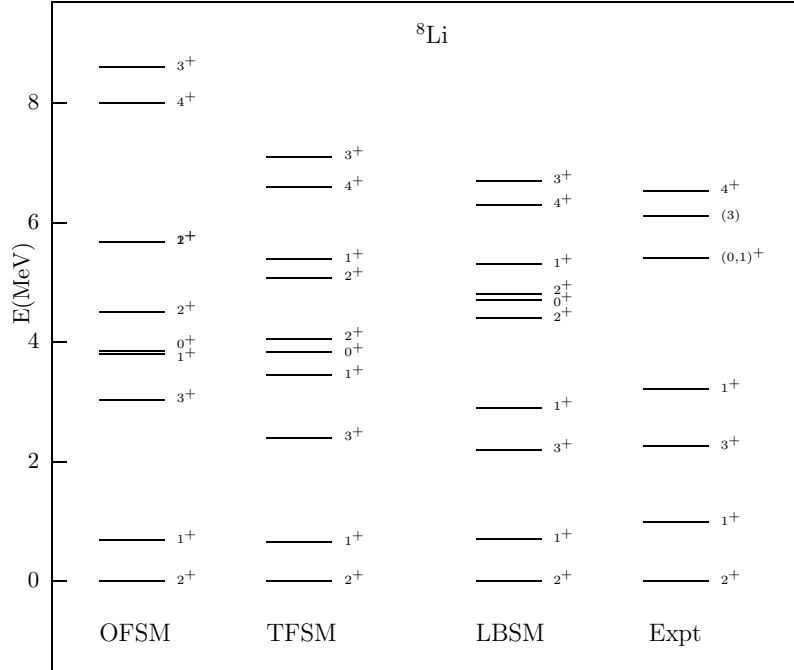


Figure 1. Experimental and calculated spectra of ${}^8\text{Li}$. See text for details.

agreement, the excitation energies produced by the one-frequency calculations are significantly higher than the observed ones for most states, the discrepancy between theory and experiment ranging from 0.3 to 2.5 MeV for the 1_1^+ and the 3_2^+ , respectively. On the other hand, the agreement between the experimental and the TFMS spectrum is very good. A significant difference (about 1 MeV) occurs, in fact, only for the second 3^+ state while for all the other states the discrepancies are less than 0.3 MeV.

As regards the quality of our results, Fig. 1 shows that they are comparable to those of Ref. 4. This is quite an achievement if one considers the very large model space used in the LBSM calculations.

4 Summary

In this paper, we have reported some results of TFMS calculations for p -shell nuclei. They have been obtained by employing an effective interaction

derived from the Bonn-A nucleon-nucleon potential by means of a G -matrix folded-diagram method.

Within the framework of the TFMS, the G matrix is calculated in a space composed of wave functions of two different length parameters, one for the inner core orbits and the other for the outer valence orbits. As compared to large-basis shell-model calculations, this approach provides a convenient alternative, as it appears from the results of our calculations. The quality of these results may be taken as an indication that most of the effects which are not explicitly taken into account in our model space are included in the effective interaction.

Acknowledgments

This work was supported in part by the Italian Ministero dell'Università e della Ricerca Scientifica e Tecnologica (MURST) and by the US grant no DE-FG02-88ER40388. N.I. would like to thank the European Social Fund for financial support.

References

1. I. Tanihata *et al.*, *Phys. Rev. Lett.* **55**, 2676 (1985).
2. I. Tanihata *et al.*, *Phys. Lett. B* **160**, 380 (1985).
3. P.G. Hansen and B. Jonson, *Europhys. Lett.* **4**, 409 (1987).
4. A.A. Wolters, A.G.M. van Hees, and P.W.M. Glaudemans, *Phys. Rev. C* **42**, 2062 (1990).
5. H. Nakada and T. Otsuka, *Phys. Rev. C* **49**, 886 (1994).
6. P. Navrátil and B.R. Barrett, *Phys. Rev. C* **57**, 3119 (1998), and references therein.
7. T.T.S. Kuo, H. Müther, and K. Amir Azimi-Nili, *Nucl. Phys. A* **606**, 15 (1996).
8. T.T.S. Kuo, F. Krmpotić, and Y. Tzeng, *Phys. Rev. Lett.* **78**, 2708 (1997).
9. T.T.S. Kuo, in *New Perspectives in Nuclear Structure*, ed. A. Covello (World Scientific, Singapore, 1996), p. 131.
10. T.T.S. Kuo, *Lecture Notes in Physics* Vol. 482 (Springer-Verlag, Berlin, 1997), p. 25.
11. E.M. Krencigłowa, C.L. Kung, T.T.S. Kuo, and E. Osnes, *Ann. Phys. (N.Y.)* **101**, 154 (1976).
12. S.F. Tsai and T.T.S. Kuo, *Phys. Lett. B* **39**, 427 (1972).
13. T.T.S. Kuo and E.M. Krencigłowa, *Nucl. Phys. A* **342**, 454 (1980).

14. K. Suzuki and S.Y. Lee, *Prog. Theor. Phys.* **64**, 2091 (1980).
15. J. Shurpin, T.T.S. Kuo, and D. Strottman, *Nucl. Phys. A* **408**, 310 (1983).
16. M. Hjorth-Jensen, T.T.S. Kuo, and E. Osnes, *Phys. Rep.* **261**, 126 (1995).
17. M. Hjorth-Jensen, H. Mütter, E. Osnes, and A. Polls, *J. Phys. G* **22**, 321 (1996).
18. B.A. Brown, A. Etchegoyen, and W.D.M. Rae, *The computer code OXBASH*, MSU-NSCL Report Number 524.
19. NNDC On-Line Data Service from the ENSDF database.
20. G. Audi and A.H. Wapstra, *Nucl. Phys. A* **595**, 409 (1995).
21. R. Machleidt, *Adv. Nucl. Phys.* **19**, 189 (1989).
22. A.A. Wolters, A.G.M. van Hees, and P.W.M. Glaudemans, *Phys. Rev. C* **42**, 2053 (1990).
23. L. Coraggio, A. Covello, A. Gargano, N. Itaco, and T.T.S. Kuo, to be published.
24. T.T.S. Kuo, L. Coraggio, A. Covello, and A. Gargano, in *Highlights of Modern Nuclear Structure*, ed. A. Covello (World Scientific, Singapore, 1999), p. 105.